

PAPER

An Algorithm for Single Snapshot 2D-DOA Estimation Based on a Three-Parallel Linear Array Model

Shiwen LIN^{†a)}, Yawen ZHOU^{†b)}, Weiqin ZOU^{†c)}, Huaguo ZHANG^{†d)}, Lin GAO^{†e)}, *Nonmembers*,
Hongshu LIAO^{†f)}, *Member*, and Wanchun LI^{†g)}, *Nonmember*

SUMMARY Estimating the spatial parameters of the signals by using the effective data of a single snapshot is essential in the field of reconnaissance and confrontation. Major drawback of existing algorithms is that its constructed covariance matrix has a great degree of rank loss. The performance of existing algorithms gets degraded with low signal-to-noise ratio. In this paper, a three-parallel linear array based algorithm is proposed to achieve two-dimensional direction of arrival estimates in a single snapshot scenario. The key points of the proposed algorithm are: 1) construct three pseudo matrices with full rank and no rank loss by using the single snapshot data from the received signal model; 2) by using the rotation relation between pseudo matrices, the matched 2D-DOA is obtained with an efficient parameter matching method. Main objective of this work is on improving the angle estimation accuracy and reducing the loss of degree of freedom in single snapshot 2D-DOA estimation.

key words: *three-parallel linear array model, single snapshot, 2D-DOA estimation, parameter matching, rotation invariance*

1. Introduction

The estimation of 2D-DOA has received a significant amount of attention over the last several decades. It is a key problem in array signals processing such as mobile communication systems [1], MIMO radar [2], [3], and remote sensing [4]. Many prominent algorithms, such as multiple signal classification (MUSIC) [5] and estimation of signal parameters via rotation invariance techniques (ESPRIT) [6], have been developed over the years and extended to 2D-DOA estimation [7]–[9]. Many signal source localization has focused on the scene of DOA estimation for an instantaneous signal with a limited single snapshot. However, the traditional method finds little application in such a scene because the subspace cannot be accurately divided due to insufficient data in a single snapshot [10]–[12]. The problem is analyzed as follows: In a single snapshot, the rank of the covariance matrix of the array is only 1, which will cause “rank loss,” that is, the rank is less than the number of

sources. Due to the extremely small amount of data and the “rank loss” problem, the two subspaces cannot be accurately divided to achieve 2D-DOA estimation.

From a practical viewpoint, major studies on solving the problem of 2D-DOA estimation in a single snapshot have been focused on realizing the restoration of the covariance matrix rank. By using the spatial smoothing method, A. Thakre et al. [13] estimated the DOA of sources by achieving the restoration of the rank of the data covariance matrix. B. F. Jiang et al. [14] achieved DOA estimation through the construction of weighted summation of single snapshot data received by antenna arrays. Q. S. Ren et al. [15] extended MUSIC to single snapshot and realized matrix rank restoration by constructing pseudo-covariance matrix. Even though the above methods in [13]–[15] work well for realizing the restoration of the covariance matrix rank, they essentially use the loss of degrees of freedom to make up for the “rank loss,” and they will result in a reduction in the maximum number of sources in DOA estimates. Y. Wu et al. [16] used a uniform rectangular array (URA) to accomplish joint estimation of the azimuth and elevation angles. It uses the particularity of the URA structure and automatically matches 2D angles through the calculation of an iterative procedure which utilizes the sinusoidal linear prediction (LP) property and weighted least squares (WLS). But this method also has a problem of large loss of degrees of freedom, and its number of sources can be estimated is strictly limited by the number of elements of the rectangular side length. Dakulagi, V [17] proposed a single snapshot 2D-DOA estimation by using a UCA-DOA. It uses the doublet structure array antenna consist of UCA array and the mode-space transformation method to realize the two-dimensional angle measurement in the single snapshot scene. However, this method still has a large loss of freedom due to the mode-space transformation process.

Q. Lin et al. [18] proposed a single snapshot two-dimensional DOA estimation method based on parallel linear arrays, which calculates the two-dimensional angle by reconstructing the matrix through multiple non-rank loss pseudo-covariance matrices and using the ESPRIT method. However, this method is based on a strictly non-circular signal with zero initial phases, and this signal has been proved to be almost impossible in practice [19], [20]. To address the limitation of non-circular signals, L. Wang et al. [21] offered a single snapshot DOA matrix method (SS-DOAM) based on parallel linear arrays to achieve two-dimensional

Manuscript received June 28, 2021.

Manuscript revised September 6, 2021.

Manuscript publicized October 5, 2021.

[†]The authors are with School of Electronic Engineering, University of Electronic Science and Technology of China, Chengdu 611731, P.R. China.

a) E-mail: 201922011430@std.uestc.edu.cn

b) E-mail: a.carolzou@gmail.com

c) E-mail: wqzou@outlook.com

d) E-mail: uestczhanghuaguo@uestc.edu.cn

e) E-mail: lingao_1014@126.com

f) E-mail: hsliao@uestc.edu.cn

g) E-mail: liwanchun@uestc.edu.cn

DOI: 10.1587/transfun.2021EAP1074

DOA estimation. However, the method has the limitation that the number of linear array elements must be odd numbers, and there is a large loss of degrees of freedom.

This paper proposes an effective method for 2D-DOA estimation in a single snapshot to overcome the above problems. First, the proposed method designs three-parallel linear arrays to form a signal receiving array. Then, three pseudo-matrices with full rank and no rank loss are constructed by using the single snapshot data of the array. Finally, the direction of arrival can be estimated by matching joint parameter, which is obtained by singular value decomposition of the matrix composed of three pseudo-matrices. The algorithm can effectively reduce the loss of degrees of freedom in the implementation process. Simulations show that the proposed method can provide better DOA estimation accuracy than the SS-DOAM method in [21], especially under scenarios of low signal-to-noise ratio (SNR).

Throughout the paper, italic small letters, boldface small letters, and boldface capital letters are used for scalars, vectors, and matrices, respectively. $(\cdot)^T$, $(\cdot)^H$ and $(\cdot)^*$ denotes transpose, Hermitian transpose, and the complex conjugate of the operand.

2. Algorithm Description

2.1 Signal Receiving Model Composed of a Three-Parallel Linear Array

As shown in Fig. 1, the antenna array consists of three parallel linear arrays in the xy -plane. The subarray 1, 2, and 3 have M , $M + 1$ and M receiving antennas respectively. Each element has the same signal response characteristics, and the elements numbered from 0 to M are parallel. The distance between sub-array elements is the same, and the distance between the elements is d .

The signal receiving model is shown in Fig. 2. Suppose N far-field narrowband signals impinge on the antenna array in the presence of white Gaussian noise. Denote by s_i the i th incident signal, φ_i its elevation angle, and θ_i its azimuth angle, ($\theta \in (-\pi, \pi)$, $\varphi \in (0, \pi/2)$, $i = 1, 2, \dots, N$). Suppose these signals have the same center frequency and the signal wavelength λ is not less than $2d$. Denote by x_i the i th element in subarray 3, y_i the i th element in subarray 2, z_i the i th element in subarray 1. The element placed at the origin is common for referencing purposes. Then the steering vectors of each subarray can be expressed as:

$$\mathbf{a}_1(\theta_i, \varphi_i) = [e^{\frac{2\pi d}{\lambda}(\cos \theta_i \sin \varphi_i)}, \dots, e^{-\frac{2\pi d}{\lambda}(m \cdot \sin \theta_i \sin \varphi_i - \cos \theta_i \sin \varphi_i)}, \dots, e^{-\frac{2\pi d}{\lambda}((M-1) \cdot \sin \theta_i \sin \varphi_i - \cos \theta_i \sin \varphi_i)}]^T \quad (1)$$

$$\mathbf{a}_2(\theta_i, \varphi_i) = [1, \dots, e^{-\frac{2\pi d}{\lambda}m \cdot \sin \theta_i \sin \varphi_i}, \dots, e^{-\frac{2\pi d}{\lambda}M \cdot \sin \theta_i \sin \varphi_i}]^T \quad (2)$$

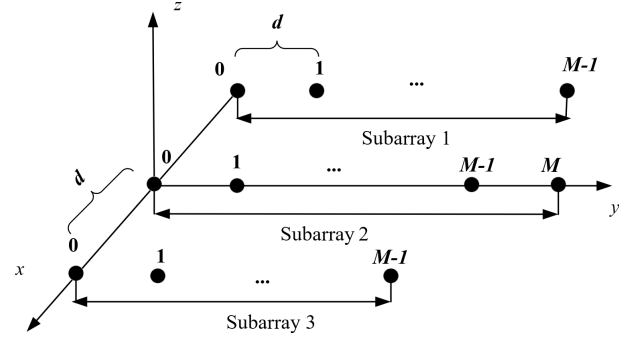


Fig. 1 Structure diagram of three-parallel linear array.

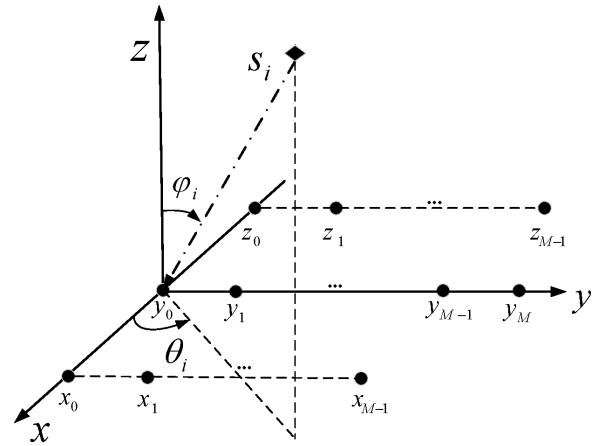


Fig. 2 Schematic diagram of signal receiving model.

$$\mathbf{a}_3(\theta_i, \varphi_i) = [e^{-\frac{2\pi d}{\lambda}(\cos \theta_i \sin \varphi_i)}, \dots, e^{-\frac{2\pi d}{\lambda}(m \cdot \sin \theta_i \sin \varphi_i + \cos \theta_i \sin \varphi_i)}, \dots, e^{-\frac{2\pi d}{\lambda}((M-1) \cdot \sin \theta_i \sin \varphi_i + \cos \theta_i \sin \varphi_i)}]^T \quad (3)$$

Accordingly, the single snapshot signal data matrix obtained by the three-parallel linear arrays can be given by:

$$\mathbf{W}_x = [x_0, x_1, \dots, x_{M-1}]^T = \mathbf{A}_1 \mathbf{S} + \mathbf{N}_1 \quad (4)$$

$$\mathbf{W}_y = [y_0, y_1, \dots, y_{M-1}, y_M]^T = \mathbf{A}_2 \mathbf{S} + \mathbf{N}_2 \quad (5)$$

$$\mathbf{W}_z = [z_0, z_1, \dots, z_{M-1}]^T = \mathbf{A}_3 \mathbf{S} + \mathbf{N}_3 \quad (6)$$

where \mathbf{A}_1 , \mathbf{A}_2 , and \mathbf{A}_3 are the subarray manifold, $\mathbf{S} = [s_1, s_2, \dots, s_N]^T$ is the single snapshot signal from different directions and \mathbf{N}_1 , \mathbf{N}_2 , \mathbf{N}_3 represent the additive white Gaussian noise (AWGN).

2.2 Construct Pseudo-Matrix

According to the single snapshot data received the designed array, we construct three pseudo-matrices, and the form of these pseudo-matrices is as follows:

$$\mathbf{R}_1 = \begin{bmatrix} y_0 y_0^* & y_1^* y_0 & y_2^* y_0 & \cdots & y_{M-1}^* y_0 \\ y_1 y_0^* & y_0 y_0^* & y_1 y_0^* & \cdots & y_{M-2}^* y_0 \\ \vdots & \vdots & \vdots & \ddots & \vdots \\ y_{M-1} y_0^* & y_{M-2} y_0^* & y_{M-3} y_0^* & \cdots & y_0 y_0^* \end{bmatrix} \quad (7)$$

$$\mathbf{R}_2 = \begin{bmatrix} y_1 y_0^* & y_0^* y_0 & y_1^* y_0 & \cdots & y_{M-2}^* y_0 \\ y_2 y_0^* & y_1 y_0^* & y_0 y_0^* & \cdots & y_{M-3}^* y_0 \\ \vdots & \vdots & \vdots & \ddots & \vdots \\ y_M y_0^* & y_{M-1} y_0^* & y_{M-2} y_0^* & \cdots & y_1 y_0^* \end{bmatrix} \quad (8)$$

$$\mathbf{R}_3 = \begin{bmatrix} z_0 y_0^* & x_1^* y_0 & x_2^* y_0 & \cdots & x_{M-1}^* y_0 \\ z_1 y_0^* & z_0 y_0^* & x_1^* y_0 & \cdots & x_{M-2}^* y_0 \\ \vdots & \vdots & \vdots & \ddots & \vdots \\ z_{M-1} y_0^* & z_{M-2} y_0^* & z_{M-3} y_0^* & \cdots & z_0 y_0^* \end{bmatrix} \quad (9)$$

The constructed three pseudo-matrices are all M -dimensional square matrices. To simplify the representation, we define k for rows and q for columns ($k, q \in (1, 2, \dots, M)$), $u_i = \exp\{-2\pi d/\lambda \sin \theta_i \sin \varphi_i\}$, $v_i = \exp\{-2\pi d/\lambda \cos \theta_i \sin \varphi_i\}$, σ_n^2 is the variance of AWGN. Then, the elements of the k th row and the q th column of the three pseudo-matrices can be respectively expressed as:

$$\mathbf{R}_1(k, q) = \begin{cases} y_{q-k}^* y_0 = \sum_{i=1}^N \sum_{j=1}^N u_i^k s_j s_i^* (u_i^q)^* + \sigma_n^2 \delta(q-k), q > k \\ y_{k-q} y_0^* = \sum_{i=1}^N \sum_{j=1}^N u_j^k s_j s_i^* (u_i^q)^* + \sigma_n^2 \delta(k-q), k \geq q \end{cases} \quad (10)$$

$$\mathbf{R}_2(k, q) = \begin{cases} y_{q-k-1}^* y_0 = \sum_{i=1}^N \sum_{j=1}^N u_i^{k+1} s_j s_i^* (u_i^q)^* + \sigma_n^2 \delta(q-k-1), q > k \\ y_{k-q+1} y_0^* = \sum_{i=1}^N \sum_{j=1}^N u_j^{k+1} s_j s_i^* (u_i^q)^* + \sigma_n^2 \delta(k-q-1), k \geq q \end{cases} \quad (11)$$

$$\mathbf{R}_3(k, q) = \begin{cases} x_{q-k}^* y_0 = \sum_{i=1}^N \sum_{j=1}^N v_i u_i^k s_j s_i^* (u_i^q)^*, q > k \\ z_{k-q} y_0^* = \sum_{i=1}^N \sum_{j=1}^N v_i u_j^k s_j s_i^* (u_i^q)^*, k \geq q \end{cases} \quad (12)$$

According to (10)–(12), three pseudo-matrix vector expression forms can be written as:

$$\mathbf{R}_1 = \mathbf{A}_M \mathbf{R}_{SS} \mathbf{A}_M^H + \sigma_n^2 \mathbf{I}_M \quad (13)$$

$$\mathbf{R}_2 = \mathbf{A}_M \mathbf{\Phi}_1 \mathbf{R}_{SS} \mathbf{A}_M^H + \sigma_n^2 \mathbf{J}_M^T \quad (14)$$

$$\mathbf{R}_3 = \mathbf{A}_M \mathbf{\Phi}_2 \mathbf{R}_{SS} \mathbf{A}_M^H \quad (15)$$

where

$$\mathbf{\Phi}_1 = \text{diag} \left(e^{-\frac{2\pi d}{\lambda} \sin \theta_1 \sin \varphi_1}, e^{-\frac{2\pi d}{\lambda} \sin \theta_2 \sin \varphi_2}, \dots, e^{-\frac{2\pi d}{\lambda} \sin \theta_N \sin \varphi_N} \right) \quad (16)$$

$$\mathbf{\Phi}_2 = \text{diag} \left(e^{-\frac{2\pi d}{\lambda} \cos \theta_1 \sin \varphi_1}, e^{-\frac{2\pi d}{\lambda} \cos \theta_2 \sin \varphi_2}, \dots, e^{-\frac{2\pi d}{\lambda} \cos \theta_N \sin \varphi_N} \right) \quad (17)$$

$$\mathbf{R}_{SS} = \text{diag} \left(s_1^* \sum_{i=1}^N s_i, s_2^* \sum_{i=1}^N s_i, \dots, s_N^* \sum_{i=1}^N s_i \right) \quad (18)$$

$$\mathbf{J}_M = \begin{bmatrix} 0 & 0 \\ \mathbf{I}_{M-1} & 0 \end{bmatrix}_{M \times M} \quad (19)$$

\mathbf{I}_M in (13) is the M -dimensional unit matrix and \mathbf{A}_M is the array manifold matrix of the array composed of the

first M elements of the subarray 2. $\mathbf{\Phi}_1$ and $\mathbf{\Phi}_2$ are both N -dimensional full-rank diagonal matrices. The rank of \mathbf{R}_{SS} is equal to the number of sources in the single snapshot scene, it realizes the restoration of the covariance matrix rank. As a result, the three pseudo-matrices \mathbf{R}_1 , \mathbf{R}_2 , and \mathbf{R}_3 must be full-rank matrices and the rank of the matrix is M .

A large matrix $\bar{\mathbf{R}}$ is constructed by using the three pseudo-matrices, and the construction form is written as:

$$\bar{\mathbf{R}} = \begin{bmatrix} \mathbf{R}_1 \\ \mathbf{R}_2 \\ \mathbf{R}_3 \end{bmatrix} = \begin{bmatrix} \mathbf{A}_M \\ \mathbf{A}_M \mathbf{\Phi}_1 \\ \mathbf{A}_M \mathbf{\Phi}_2 \end{bmatrix} \mathbf{R}_{SS} \mathbf{A}_M^H + \sigma_n^2 \begin{bmatrix} \mathbf{I}_M \\ \mathbf{J}_M^T \\ \mathbf{O}_M \end{bmatrix} \quad (20)$$

\mathbf{O}_M is an M -dimensional zero matrix.

2.3 ESPRIT-Based Two-Dimensional Angle Parameter Pairing

By performing singular value decomposition on the matrix $\bar{\mathbf{R}}$, the signal subspace \mathbf{E}_S can be obtained as:

$$\mathbf{E}_S = \begin{bmatrix} \mathbf{E}_1 \\ \mathbf{E}_2 \\ \mathbf{E}_3 \end{bmatrix} = \begin{bmatrix} \mathbf{A}_M \mathbf{T} \\ \mathbf{A}_M \mathbf{\Phi}_1 \mathbf{T} \\ \mathbf{A}_M \mathbf{\Phi}_2 \mathbf{T} \end{bmatrix} \quad (21)$$

Since \mathbf{T} is an N -dimensional invertible matrix, a least-squares problem based on LS-ESPRIT [22] can be established as:

$$\min \left\| \begin{bmatrix} \mathbf{E}_1 \\ \mathbf{E}_2 \\ \mathbf{E}_3 \end{bmatrix} - \begin{bmatrix} \mathbf{A}_M \mathbf{T} \\ \mathbf{A}_M \mathbf{\Phi}_1 \mathbf{T} \\ \mathbf{A}_M \mathbf{\Phi}_2 \mathbf{T} \end{bmatrix} \right\|_F^2 = \min \|\mathbf{E}_S - \bar{\mathbf{A}} \mathbf{T}\|^2 \quad (22)$$

By solving the least square solution of (22), the rotation matrix $\mathbf{\Psi}_1$ and $\mathbf{\Psi}_2$ are obtained as:

$$\begin{cases} \mathbf{\Psi}_1 = \mathbf{T}^{-1} \mathbf{\Phi}_1 \mathbf{T} = (\mathbf{E}_1^H \mathbf{E}_1)^{-1} \mathbf{E}_1^H \mathbf{E}_2 \\ \mathbf{\Psi}_2 = \mathbf{T}^{-1} \mathbf{\Phi}_2 \mathbf{T} = (\mathbf{E}_1^H \mathbf{E}_1)^{-1} \mathbf{E}_1^H \mathbf{E}_3 \end{cases} \quad (23)$$

Since the matrix $\mathbf{\Phi}_1$ and $\mathbf{\Phi}_2$ in (20) contain the DOA information of all input signals, The two eigenvalue diagonal matrices obtained by eigen decomposition of the rotation matrices $\mathbf{\Psi}_1$ and $\mathbf{\Psi}_2$ respectively still contain the angle parameter information of the signal. However, since the eigen-decomposition process of $\mathbf{\Psi}_1$ and $\mathbf{\Psi}_2$ is independent, it is necessary to determine the correspondence between the eigenvalues of the two matrices to complete the two-dimensional angle parameter pairing. The parameter matching process is as follows:

Perform eigen-decomposition on the rotation matrices \mathbf{A} and \mathbf{B} , respectively, and we can get $\mathbf{\Psi}_1$ and $\mathbf{\Psi}_2$ as:

$$\mathbf{\Psi}_1 = \mathbf{T}_1 \mathbf{\Phi}_1 \mathbf{T}_1^{-1} = \mathbf{T}_1 \begin{bmatrix} \lambda_1 & & \\ & \ddots & \\ & & \lambda_N \end{bmatrix} \mathbf{T}_1^{-1} \quad (24)$$

$$\Psi_2 = \mathbf{T}_2 \Phi_2 \mathbf{T}_2^{-1} = \mathbf{T}_2 \begin{bmatrix} \gamma_1 & & \\ & \ddots & \\ & & \gamma_N \end{bmatrix} \mathbf{T}_2^{-1} \quad (25)$$

where \mathbf{T}_1 is the eigenvector matrix obtained by eigen-decomposition of matrix Ψ_1 ; $\lambda_1, \dots, \lambda_N$ represents the eigenvalue of matrix Ψ_1 ; \mathbf{T}_2 is the eigenvector matrix obtained by eigen-decomposition of matrix Ψ_2 ; $\gamma_1, \dots, \gamma_N$ represents the eigenvalue of matrix Ψ_2 .

Calculate the phase angle of the eigenvalue $\gamma_1, \dots, \gamma_N$, and sort them from large to small according to the size of their phase angle, and obtain the sorted eigenvalues $\gamma_1, \dots, \gamma_N$. Then, use the eigenvector matrix \mathbf{T}_1 to get the estimated matrix $\hat{\Phi}_2$ of the eigenvalue matrix $\hat{\Phi}_2$ as follows:

$$\hat{\Phi}_2 = \mathbf{T}_1^{-1} \Psi_2 \mathbf{T}_1 \quad (26)$$

Define u_1, \dots, u_N are the diagonal elements of $\hat{\Phi}_2$. Take complex phase angles for all diagonal elements, and sort them from large to small according to the size of their phase angle to obtain the sorted eigenvalues $\bar{u}_1, \dots, \bar{u}_N$. Then, there is a pairing relationship as:

$$\bar{\gamma}_i = \bar{u}_i, i = 1, 2, \dots, N \quad (27)$$

Adjust the eigenvalue order of Ψ_1 through the relationship between the diagonal elements $\bar{u}_1, \dots, \bar{u}_N$ and its corresponding feature vector to obtain the sorted eigenvalues $\bar{\lambda}_1, \dots, \bar{\lambda}_N$. Then, we can get the eigenvalue pairing relationship as:

$$\bar{\gamma}_i = \bar{\lambda}_i, i = 1, 2, \dots, N \quad (28)$$

According to the eigenvalue pairing relationship to complete the angle parameter pairing, the solution of 2D-DOA of sources is obtained in (29) as [23]. “ \angle ” is the symbol of the complex number to obtain the phase angle.

$$\begin{cases} \hat{\theta}_i^{Fuzzy} = \arctan \left[\frac{\angle \bar{\lambda}_i}{\angle \bar{\gamma}_i} \right] \\ \hat{\varphi}_i = \arcsin \left[\frac{\lambda \sqrt{(\angle \bar{\lambda}_i)^2 + (\angle \bar{\gamma}_i)^2}}{2\pi d} \right] \end{cases} \quad (29)$$

Since the azimuth angle calculated by the arctangent function is $\hat{\theta}_i^{Fuzzy} \in (-\pi/2, \pi/2)$, the azimuth angle is blurred in this signal model. This paper defuzzifies the azimuth angle in (30) by using the positive and negative of the eigenvalue. The accurate direction of arrival estimates can be obtained by (29) and (30).

$$\begin{cases} \hat{\theta}_i = \hat{\theta}_i^{Fuzzy} + \frac{k_i \pi}{2} \\ k_i = \text{sign}(\angle \bar{\lambda}_i) (1 - \text{sign}(\angle \bar{\gamma}_i)) \end{cases} \quad (30)$$

2.4 Algorithm Steps

The steps of this algorithm for single snap-shot 2D-DOA estimation based on the three-parallel linear array are as follows:

- (i) Construct three pseudo-matrices from the single snapshot data received by the array in (7)–(9).
- (ii) Construct a large matrix $\bar{\mathbf{R}}$ by using the three pseudo-matrices in (20).
- (iii) Perform singular value decomposition on matrix $\bar{\mathbf{R}}$ to obtain an estimate of the signal subspace as (21).
- (iv) Obtain the least square solution of two rotation matrices Using rotation invariance Ψ_1 and Ψ_2 by using their rotation invariance in (23).
- (v) Determine the correspondence between the eigenvalues of Ψ_1 and Ψ_2 , and complete the angle parameter pairing.
- (vi) Calculate the azimuth angle and the elevation angle in (29) and (30).

3. Algorithm Analysis and Simulation

3.1 Degrees of Freedom of the Algorithm

In this section, we evaluated the loss of the algorithm's degree of freedom. The loss is $\lfloor M/2 \rfloor$ under the SS-DOAM method, and its ratio of the degree of freedom to the size of the corresponding arrays is $\lfloor M/2 \rfloor / (2M + 1)$. By the constructed three-parallel linear array and the proposed algorithm, the ratio of the degree of freedom to the number of all elements turns to $M/(3M+1)$. Obviously, because of $M \geq 2$, the algorithm has less loss of freedom than the SS-DOAM method. It clearly proves that the proposed algorithm can effectively reduce the loss of the degree of freedom.

3.2 Computational Complexity Analysis

The computational complexity of the sparse arrays is analyzed in this section. First, we construct three pseudo-covariance matrices in (7)–(9) with complexity $O(3M^2)$. Then, we perform singular value decomposition on the constructed pseudo-matrix in (20) and the complexity of the process is $O(27M^3)$. The computational complexity required for the process to obtain the least square solution of two rotation matrices in (22)–(26) is $O(2N^3 + 6MN^2)$. Finally, The computational complexity required for the two-dimensional angle parameter solving and matching process in (29), (30) is $O(3N^3)$.

In summary, the computational complexity of the proposed method is $O(27M^3 + 5N^3 + 6MN^2 + 3M^2)$ and it mainly depends on computation of pseudo-covariance matrices, eigen value decomposition, finding solutions of invariance equations and 2D-DOA estimation.

3.3 Simulation Results

In this section, simulations are presented to illustrate the

proposed method in single snapshot 2D-DOA estimation. Results on each of the simulations were analyzed with 1000 independent trials.

The statistical performance of the algorithm is evaluated by the mean square error (RMSE) of the angle estimate, and the mean square error of the two-dimensional angle estimate is defined as:

$$\begin{aligned} \text{RMSE}(\theta, \varphi) &= \sqrt{E[(\hat{\theta}_k - \theta)^2] + E[(\hat{\varphi}_k - \varphi)^2]} \\ &= \sqrt{\frac{1}{K} \sum_{k=1}^K (\hat{\theta}_k - \theta)^2 + (\hat{\varphi}_k - \varphi)^2} \end{aligned} \quad (31)$$

The estimated mean square error of the azimuth angle θ is defined as:

$$\text{RMSE}(\theta) = \sqrt{E[(\hat{\theta}_k - \theta)^2]} = \sqrt{\frac{1}{K} \sum_{k=1}^K (\hat{\theta}_k - \theta)^2} \quad (32)$$

The estimated mean square error of the elevation angle ϕ is defined as:

$$\text{RMSE}(\varphi) = \sqrt{E[(\hat{\varphi}_k - \varphi)^2]} = \sqrt{\frac{1}{K} \sum_{k=1}^K (\hat{\varphi}_k - \varphi)^2} \quad (33)$$

K is the number of independent random experiments, $\hat{\varphi}_k$ is the estimated elevation angle of the k th experiment, $\hat{\theta}_k$ is the estimated azimuth angle of the k th experiment.

Simulation I: Assume that the total number of the three-parallel linear arrays is 37 and the number of subarray 1, 2, and 3 are 12, 13, and 12, respectively. The elements are separated by a half-wavelength in each subarray, i.e., element spacing $d = 0.5\lambda$. The proposed method is compared to the SS-DOAM method proposed by [21]. The number of parallel linear arrays based on the SS-DOAM method is also 37, and its two sub-array elements are 19 and 18, respectively. Three far-field narrowband signals impinge on both antenna arrays, and the angles of arrivals are $(40^\circ, 30^\circ)$, $(50^\circ, 50^\circ)$, and $(60^\circ, 30^\circ)$. The signal-to-noise ratio $SNR = 10$ dB.

The scatter diagrams of the measured DOA estimation are shown in Fig. 3 and Fig. 4. From the Fig. 3, it is clear that the estimated points of multiple independent trials form three-point “clusters” around the actual position, and there is a clear distinction between “cluster” and “cluster.” There is no clear distinction in Fig. 4. Besides, the RMSEs of Fig. 3 and Fig. 4 are 3.1521° and 7.3765° respectively. By comparing Fig. 3 and Fig. 4, it can be seen that the proposed algorithm has a better 2D-DOA estimation performance with multiple sources than the SS-DOAM method.

Simulation II: Assume that the size of the three-parallel linear arrays and parallel linear arrays remains unchanged from that of *Simulation I*. Then increase the SNR to

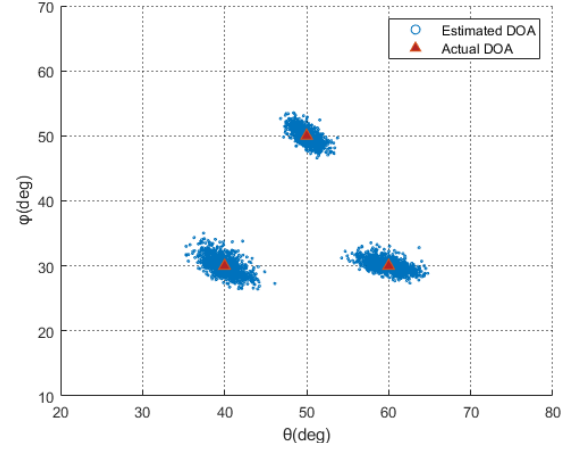


Fig. 3 The DOA estimated by the proposed method at $SNR=10$ dB.

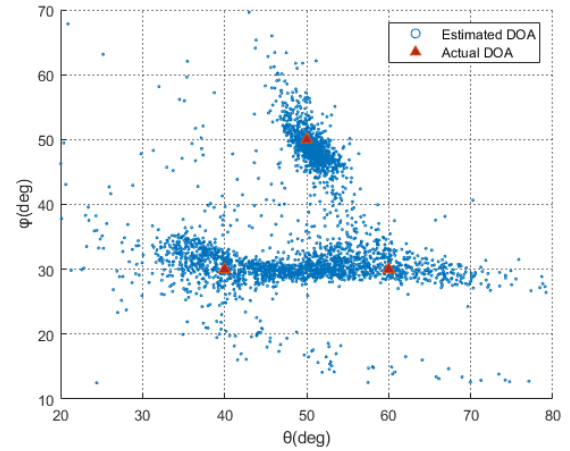


Fig. 4 The DOA estimated by the SS-DOAM method at $SNR=10$ dB.

20 dB. The result of the update is shown in Fig. 5 and Fig. 6. It is found that the estimated points are more closely aligned with the actual point and the RMSEs of Fig. 5 and Fig. 6 are 0.8572° and 2.5050° respectively. This means that the performance of the algorithm improves as the SNR increases, and the proposed method still outperforms the SS-DOAM method.

Simulation I and *Simulation II* is done based on multiple target sources. And then we do the following simulations with a single source impinging on both arrays.

Simulation III: Assume that the total number of the three-parallel linear arrays is 49 and the number of subarray 1, 2, and 3 are 16, 17, and 16, respectively. The elements are separated by a half-wavelength in each subarray, i.e., element spacing $d = 0.5\lambda$. The proposed method is compared to the SS-DOAM method proposed by [21]. The number of parallel linear arrays based on the SS-DOAM method is also 49, and its two sub-array elements are 25 and 24, respectively. There is only one far-field narrowband signal impinges on both antenna arrays, and the angle is $(45^\circ, 45^\circ)$.

The scatter diagrams of the measured DOA estimation estimated at $SNR = 10$ dB are shown in Fig. 7 and Fig. 8.

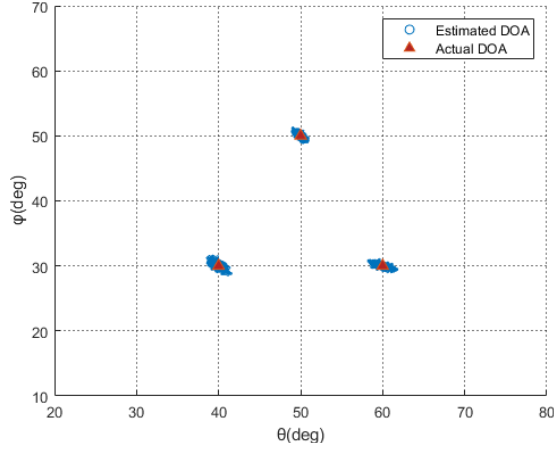


Fig. 5 The DOA estimated by the proposed method at SNR=20 dB.

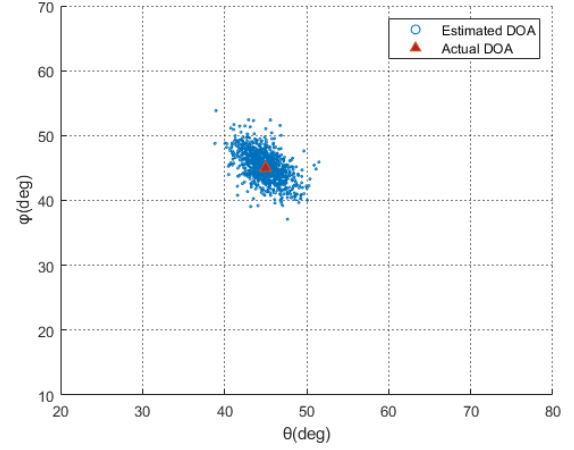


Fig. 7 The single target's DOA estimated by the proposed method at SNR=10 dB.

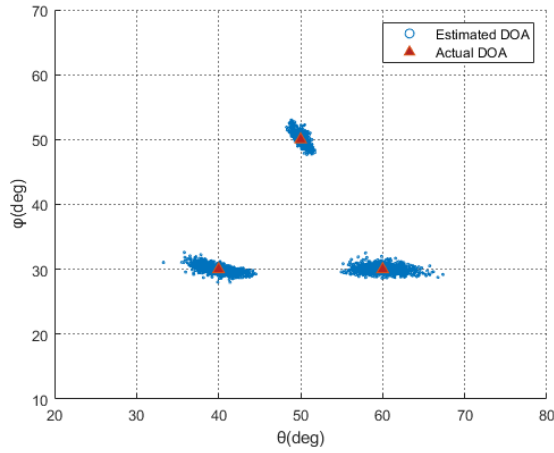


Fig. 6 The DOA estimated by the SS-DOAM method at SNR=20 dB.

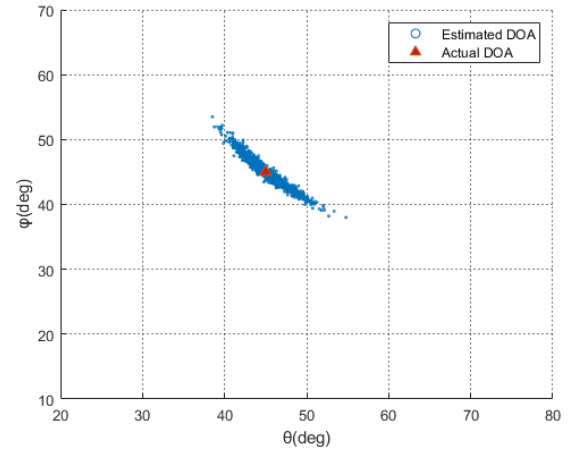


Fig. 8 The single target's DOA estimated by the SS-DOAM method at SNR=10 dB.

And the root-mean-squared errors (RMSEs) of the estimates of the elevation and azimuth DOA estimated are illustrated at different SNR in Fig. 9 and Fig. 10. As it can be seen, the proposed algorithm has a better 2D-DOA estimation performance than the SS-DOAM method, especially at low SNR.

Simulation IV: Assume that the number of elements of each sub-array in the three-parallel linear array as M . And there is only one far-field narrowband signal impinges on the array, and the angle is $(45^\circ, 45^\circ)$. The RMSEs of the estimates of 2D-DOA estimated are illustrated at different SNR in Fig. 11. In addition, Assume the total number of the three-parallel linear array used for the proposed method is equal to the total number of the parallel linear array under the SS-DOAM algorithm. As the total number of two arrays changes, we can see the performance of the two methods changes in Fig. 12.

It is clear that the 2D-DOA performance of the proposed algorithm increases as the SNR increases. And the performance becomes better when the total number of the three-parallel linear array increases. Furthermore, the proposed method outperforms the SS-DOAM with the same number of arrays.

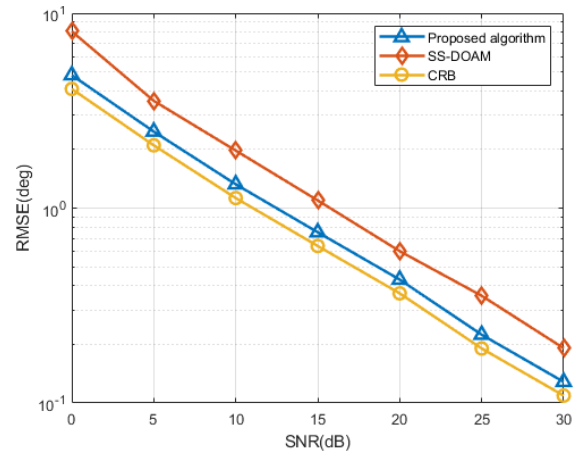


Fig. 9 The RMSE comparison for θ versus SNR of SS-DOAM and proposed method.

In summary, the proposed method outperformed the SS-DOAM method proposed by [21]. Because the proposed method takes full advantage of all received signal data of

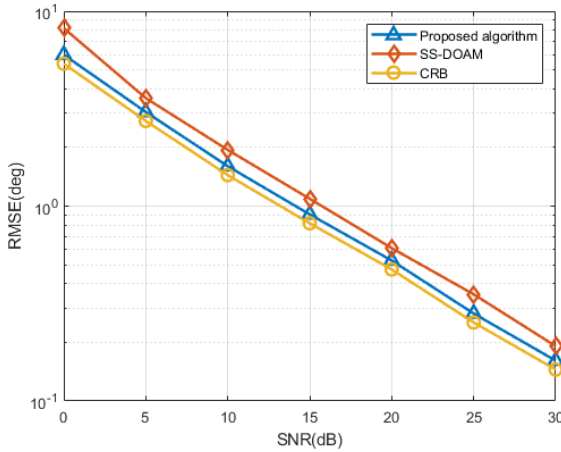


Fig. 10 The RMSE comparison for ϕ versus SNR of SS-DOAM and proposed method.

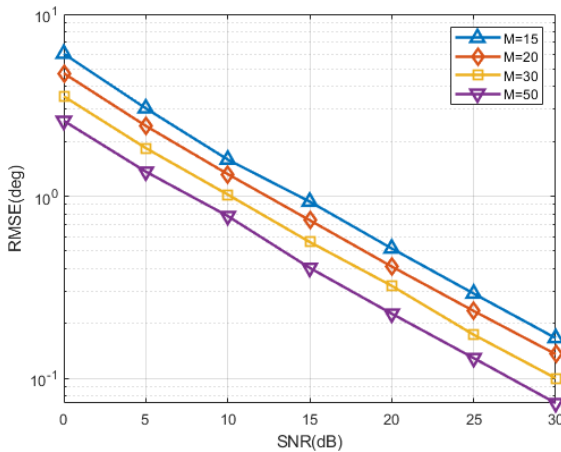


Fig. 11 The RMSE versus M of the proposed method.

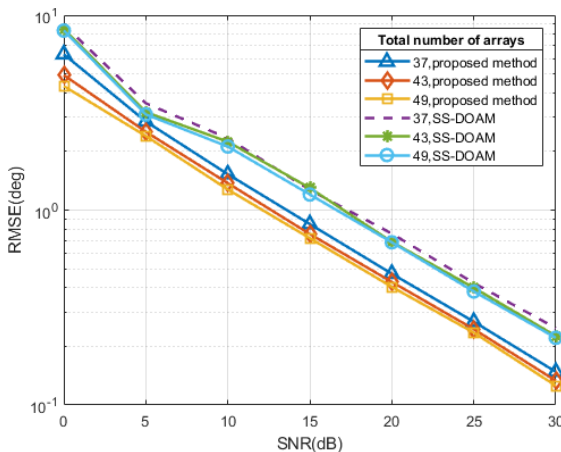


Fig. 12 The RMSE versus M of the proposed method and the SS-DOAM.

the array and effectively reduces the loss of degrees of freedom by constructing pseudo matrices and matching two-dimensional angle parameters.

4. Conclusion

In this paper, we have constructed a three-parallel linear array signal receiving model and proposed a novel method for single snapshot 2D-DOA estimation. The proposed method constructs three pseudo-matrices by using the single snapshot data of the constructed arrays. It is found that the three pseudo-matrices are full-rank matrices, and the rank is equal to the number of elements in the corresponding subarray. Then, the 2D-DOA is obtained by using the rotation invariance between the three pseudo-matrices. Compared to the SS-DOAM method, the proposed method effectively reduces the loss of the degree of freedom. Furthermore, results on simulations showed the performance for 2D-DOA estimation of the proposed method is better than the SS-DOAM method under the single snapshot scene.

5. Acknowledgments

This work was supported by National Natural Science Foundation of China (No.61971103) and Meteorological information and Signal Processing Key Laboratory of Sichuan Higher Education Institutes, PRC.

References

- [1] A.A. D'Amico and M. Morelli, "Joint channel and DOA estimation for multicarrier CDMA uplink transmissions," *IEEE Trans. Veh. Technol.*, vol.58, no.1, pp.116–125, Jan. 2009, doi: 10.1109/TVT.2008.921624.
- [2] A. Khabbazihasmenj, A. Hassanien, S.A. Vorobyov, and M.W. Morency, "Efficient transmit beamspace design for search-free based DOA estimation in MIMO radar," *IEEE Trans. Signal Process.*, vol.62, no.6, pp.1490–1500, March 2014, doi: 10.1109/TSP.2014.2299513.
- [3] P. Chen, Z. Cao, Z. Chen, and X. Wang, "Off-grid DOA estimation using sparse Bayesian learning in MIMO radar with unknown mutual coupling," *IEEE Trans. Signal Process.*, vol.67, no.1, pp.208–220, Jan. 2019, doi: 10.1109/TSP.2018.2881663.
- [4] J. Zhao, Y. Tian, B. Wen, and Z. Tian, "Coherent DOA estimation in sea surface observation with direction-finding HF radar," *IEEE Trans. Geosci. Remote Sensing*, vol.59, no.8, pp.6651–6661, 2021, doi: 10.1109/TGRS.2020.3028074.
- [5] R.O. Schmidt, "Multiple emitter location and signal parameter estimation," *IEEE Trans. Antennas Propag.*, vol.AP-34, no.3, pp.276–280, March 1986.
- [6] R. Roy and T. Kailath, "Esprit-estimation of signal parameters via rotational invariance techniques," *IEEE Trans. Acoust., Speech, Signal Process.*, vol.37, no.7, pp.984–995, July 1989.
- [7] T.-H. Liu and J.M. Mendel, "Azimuth and elevation direction finding using arbitrary array geometries," *IEEE Trans. Signal Process.*, vol.46, no.7, pp.2061–2065, July 1998, doi: 10.1109/78.700985.
- [8] Z. Ye, Y. Zhang, and X. Xu, "Two-dimensional direction of arrival estimation in the presence of uncorrelated and coherent signals," *IET Signal Process.*, vol.3, no.5, pp.416–429, 2009.
- [9] K. Tategami, M. Fujimoto, K. Kitao, and T. Imai, "2D-DOA estimation by compressed sensing using sub-arrays in an actual urban street cell environment," 2019 International Symposium on Antennas and Propagation (ISAP), pp.1–2, 2019.
- [10] B.M. Radich and K.M. Buckley, "Single-snapshot DOA estimation and source number detection," *IEEE Signal Process. Lett.*, vol.4,

- no.4, pp.109–111, April 1997, doi: 10.1109/97.566703.
- [11] J.-T. Kim, S.-H. Moon, D.S. Han, and M.-J. Cho, “Fast DOA estimation algorithm using pseudocovariance matrix,” *IEEE Trans. Antennas Propag.*, vol.53, no.4, pp.1346–1351, April 2005, doi: 10.1109/TAP.2005.844459.
- [12] A. Hassanien, M.G. Amin, Y.D. Zhang, and F. Ahmad, “High-resolution single-snapshot DOA estimation in MIMO radar with colocated antennas,” 2015 IEEE Radar Conference (RadarCon), pp.1134–1138, 2015, doi: 10.1109/RADAR.2015.7131164.
- [13] A. Thakre, M. Haardt, and K. Giridhar, “Single snapshot spatial smoothing with improved effective array aperture,” *IEEE Signal Process. Lett.*, vol.16, no.6, pp.505–508, June 2009, doi: 10.1109/LSP.2009.2017573.
- [14] B.F. Jiang, X.D. Lyu, and M.S. Xiang, “Single snapshot DOA estimation method based on rearrangement of array receiving signal,” *Journal of Electronics and Information Technology*, vol.36, no.6, pp.1334–1339, 2014.
- [15] Q.S. Ren and A.J. Willis, “Extending MUSIC to single snapshot and on line direction finding applications,” *Radar 97 (Conf. Publ. no.449)*, pp.783–787, 1997, doi: 10.1049/cp:19971783.
- [16] Y. Wu, X. Pei, and H.C. So, “Utilizing principal singular vectors for 2D DOA estimation in single snapshot case with uniform rectangular array,” *International Journal of Antennas and Propagation*, vol.2015, Article ID 681251, 6 pages, 2015.
- [17] V. Dakulagi, “Single snapshot 2D-DOA estimation in wireless location system,” *Wireless Pers. Commun.*, vol.117, pp.2327–2339, 2021.
- [18] Q. Lin, L. Huang, and P. Shuai, “Two-dimensional direction-of-arrival estimation of non-circular signals using one snapshot,” *IEEE International Geoscience and Remote Sensing Symposium (IGARSS)*, pp.4290–4293, 2016.
- [19] N. Tayem and H.M. Kwon, “Conjugate ESPRIT (C-SPRIT),” *IEEE Trans. Antennas Propag.*, vol.52, no.10, pp.2618–2624, Oct. 2004, doi: 10.1109/TAP.2004.834385.
- [20] N. Tayem and H.M. Kwon, “Reply to comments on “Conjugate ESPRIT (C-SPRIT),”,” *IEEE Tran. Antennas Propag.*, vol.55, no.2, pp.512–513, Feb. 2007, doi: 10.1109/TAP.2007.892027.
- [21] L. Wang, G.L. Li, J. Sui, and B. Deng, “Single snapshot DOA matrix method,” *Systems Engineering and Electronics*, vol.34, no.7, pp.1323–1328, 2012.
- [22] R. Roy, A. Paulraj, and T. Kailath, “ESPRIT—A subspace rotation approach to estimation of parameters of cisoids in noise,” *IEEE Trans. Acoust., Speech, Signal Process.*, vol.34, no.5, pp.1340–1342, Oct. 1986, doi: 10.1109/TASSP.1986.1164935.
- [23] L.Q. Yang, S. Liu, L.S. Yang, et al., “A new parameter matching method for 2D ESPRIT algorithm,” *Radio Engineering*, vol.44, no.11, pp.23–25+33, 2014.
- [24] P. Stoica and A. Nehorai, “MUSIC, maximum likelihood and Cramer-Rao bound: Further results and comparisons,” *International Conference on Acoustics, Speech, and Signal Processing*, vol.4, pp.2605–2608, 1989, doi: 10.1109/ICASSP.1989.267001.

Appendix: Appendices

For simplicity, we assume that the Gaussian white noise with zero mean and variance σ . The single snapshot signal data matrix shows as in Eqs.(4)–(6). Let $\mathbf{W} = [\mathbf{W}_x \ \mathbf{W}_y \ \mathbf{W}_z]^T$, $\mathbf{A} = [\mathbf{A}_1 \ \mathbf{A}_2 \ \mathbf{A}_3]^T$ and $\mathbf{N} = [\mathbf{N}_1 \ \mathbf{N}_2 \ \mathbf{N}_3]^T$. The likelihood function is expressed as:

$$\ln \mathbf{L} = \text{const} - (3M+1) \ln(\sigma) - \frac{1}{\sigma} (\mathbf{W}^H - \mathbf{S}^H \mathbf{A}^H) (\mathbf{W} - \mathbf{A} \mathbf{S}) \quad (\text{A} \cdot 1)$$

The first derivative is:

$$\begin{aligned} \frac{\partial \ln \mathbf{L}}{\partial \varphi_i} &= \frac{2}{\sigma} \text{Re}[s_i^H \mathbf{d}^H(\varphi_i) \mathbf{N}] \\ \frac{\partial \ln \mathbf{L}}{\partial \theta_i} &= \frac{2}{\sigma} \text{Re}[s_i^H \mathbf{d}^H(\theta_i) \mathbf{N}] \end{aligned} \quad (\text{A} \cdot 2)$$

where, $\mathbf{d}(\theta_i) = d\mathbf{a}_i/d\theta_i$, $\mathbf{d}(\varphi_i) = d\mathbf{a}_i/d\varphi_i$.

The Fisher information matrix is as follows:

$$\begin{aligned} \mathbf{I} &= \begin{bmatrix} \mathbf{C}' & \mathbf{U}' \\ \mathbf{V}' & \mathbf{D}' \end{bmatrix} \\ \mathbf{C}' &= \frac{2}{\sigma} \text{Re}\{\mathbf{G}^H \mathbf{D}^H(\varphi) [\mathbf{I} - \mathbf{A}(\mathbf{A}^H \mathbf{A})^{-1} \mathbf{A}^H] \mathbf{D}(\varphi) \mathbf{G}\} \\ \mathbf{D}' &= \frac{2}{\sigma} \text{Re}\{\mathbf{G}^H \mathbf{D}^H(\theta) [\mathbf{I} - \mathbf{A}(\mathbf{A}^H \mathbf{A})^{-1} \mathbf{A}^H] \mathbf{D}(\theta) \mathbf{G}\} \\ \mathbf{U}' &= \frac{2}{\sigma} \text{Re}\{\mathbf{G}^H \mathbf{D}^H(\varphi) [\mathbf{I} - \mathbf{A}(\mathbf{A}^H \mathbf{A})^{-1} \mathbf{A}^H] \mathbf{D}(\theta) \mathbf{G}\} \\ \mathbf{V}' &= \frac{2}{\sigma} \text{Re}\{\mathbf{G}^H \mathbf{D}^H(\theta) [\mathbf{I} - \mathbf{A}(\mathbf{A}^H \mathbf{A})^{-1} \mathbf{A}^H] \mathbf{D}(\varphi) \mathbf{G}\} \end{aligned} \quad (\text{A} \cdot 3)$$

where, $\mathbf{D}(\varphi) = [\mathbf{d}(\varphi_1), \dots, \mathbf{d}(\varphi_N)]$, $\mathbf{D}(\theta) = [\mathbf{d}(\theta_1), \dots, \mathbf{d}(\theta_N)]$, $\mathbf{G} = \text{diag}(s_1, \dots, s_N)$.

Then, 0CRB is expressed as:

$$\begin{aligned} \mathbf{E} &= \mathbf{I}^{-1} \\ \text{CRB}(\varphi_i) &= \mathbf{E}_{ii}, \text{CRB}(\theta_i) = \mathbf{E}_{N+i, N+i} \end{aligned} \quad (\text{A} \cdot 4)$$



Shiwen Lin was born in Sichuan, China, in 1998. He received the B.E. degree in information countermeasures from University of Electronic Science and Technology of China in 2019. He is now a graduate student in School of Information and Communication Engineering, University of Electronic Science and Technology of China.



Yawen Zhou was born in Zhengzhou, China, in 1995. She received the B.E. degree in communication engineering from Henan university in 2019. She is now a graduate student in School of Information and Communication Engineering, University of Electronic Science and Technology of China.



Weiqin Zou was born in Jiangxi, China, in 1995. He received the B.S. degree in electronic and information engineering from the University of Electronic Science and Technology of China, in 2018. He is currently a Graduate Student with the School of Information and Communication Engineering, University of Electronic Science and Technology of China.



Huaguo Zhang received the Ph.D. degree in signal and information processing from the University of Electronic Science and Technology of China, Chengdu, China, in 2011. He is currently an Associate Professor with the School of Information and Communication Engineering, University of Electronic Science and Technology of China. His current research interests include noncooperative communication signal processing and array signal processing.



Lin Gao received the B.S., M.S. and Ph.D. degrees all in information and communication engineering from the University of Electronic Science and Technology of China. From 2018 to 2020, he was a postdoc research fellow at the Department of Information Engineering of the University of Florence. Currently he is a Lecturer with the School of Information and Communication Engineering, University of Electronic Science and Technology of China. His research interests include statistical signal processing, target localization, multi-sensor multi-target tracking, information fusion and multi-vehicle SLAM.



Hongshu Liao was born in 1978. She is an associate professor of University of Electronic Science and Technology of China. Her research interests include communication signal analysis and channel code identification. She has published many papers in IET communication, Journal on Communications and other conferences, and obtained more than 10 authorized patents.



Wanchun Li was born in 1978. He received the Ph.D. degree in electronic engineering from University of Electronic Science and Technology of China (UESTC) in 2009. His research interests include passive localization and electronic countermeasure.